Copper-Free Click Chemistry Modification of Nanovectors For Integrin Targeted Cancer Therapy (Book Chapter)

Wang, Chang-Fang

Springer Science+Business Media
2018

Wang , C-F & Santos , H A 2018 , Copper-Free Click Chemistry Modification of Nanovectors For Integrin Targeted Cancer Therapy (Book Chapter) . in E Patsenker (ed.) , Integrin Targeting Systems for Tumor Diagnosis and Therapy . Methods in Pharmacology and Toxicology , Springer Science+Business Media , New York , pp. 35-49 . https://doi.org/10.1007/7653_2015_44

http://hdl.handle.net/10138/327359
https://doi.org/10.1007/7653_2015_44

acceptedVersion

ology and Toxicology
DOI 10.1007/7653_2015_44

Copper-Free Click Chemistry Modification of Nanovectors for Integrin-Targeted Cancer Therapy

Chang-Fang Wang and Hélder A. Santos

Abstract

Strain-promoted azide-alkyne cycloaddition (SPAAC) click chemistry is the chemical reaction between azide and cyclooctyne groups. This reaction can conjugate biological molecules, such as peptides, in a highly selective way under mild conditions without cross-reaction with the most widely existing reactive groups, such as amine, carboxylic acid, and hydroxide. Thus, the SPAAC reaction is very versatile for biomolecules conjugation. In this book chapter, we provide detailed protocols of conjugation of integrin targeting peptides to either amine or carboxylic acid terminated porous silicon nanovectors by SPAAC, which can be used to enhance the cellular uptake for intracellular cancer drug delivery and for in vivo cancer theranostics.

Keywords: Copper-free click chemistry, Peptide conjugation, Integrin, Targeting drug delivery, Nanomedicine, Cancer therapy

1 Introduction

One of the hallmarks of cancer is induction of angiogenesis [1]. Neovascularization plays a crucial role in the development and formation of cancer. Cancer tissue, similarly to normal tissues, requires sustaining nutrients and oxygen, eliminating metabolic waste and carbon dioxide. When the neovascularization is switched on due to the aggressive proliferation of cancer cells, the angiogenesis is in most cases activated and remains on, while in healthy subjects, the angiogenesis is only turned on by embryogenesis or wound healing and is only transiently [2].

During neovascularization, tumor angiogenic vessels express biomarkers that are not present in resting blood vessels of normal tissues [3]. The numbers of cell-specific epitopes and biomarkers, such as vascular endothelial growth factor receptors, integrins, and aminopeptidase-N protein, have been explored to show specific binding by certain antibodies, peptides, or small molecules [4]. These differentially expressed biomarkers can be used as docking sites accumulating drug molecules and/or drug carriers at the tumor tissue, namely targeting drug delivery. Integrins are one of the key types of regulators of angiogenesis, and particularly

$\alpha v\beta 3$ integrin is the most abundantly expressed by neovascular endothelial cells during angiogenesis and tumor progression, but is not present in normal quiescent endothelial cells [5]. Beside integrin $\alpha v\beta 3$, integrin $\alpha v\beta 5$ functions with vascular endothelial growth factor or transforming growth factor α to induce angiogenesis [6].

The three-amino acid peptide arginine-glycine-aspartic acid (RGD) was identified as a ligand for integrin $\alpha v\beta 3$, $\alpha v\beta 5$, and $\alpha 5\beta 1$ [7, 8]. Intravenously administrated RGD-targeted nanovectors are capable to deliver the payloads to tumor sprouting tissue while sparing the healthy tissues [9]. RGD-modified nanoparticles have been shown to accumulate within the tumor-associated blood vessels, but have been shown to bind weakly to other vascular beds [10, 11]. iRGD is a disulfide-based nine-amino acid cyclized RGD derivative peptide identified by phage display as a tumor-targeting and tissue-penetrating peptide [12]. It can first associate with tumor cells by specific affinity to $\alpha v\beta 3/5$ integrins on tumor endothelium. On the endothelia cell membrane, iRGD is cleaved between lysine (K)/arginine (R) and glycine (G) by proteolysis to produce a C-terminal motif, which can form protein neuropilin-1-mediated cell internalization. iRGD surface-modified nanovectors can include both tumor-targeting and tissue-penetrating properties for drug delivery applications and cancer therapy.

Nanovector-based drug delivery systems (DDSs) have become a hot research area in modern science, and an enormous research effort has been paid attention in the last decades to develop nanoparticulate DDSs for cancer therapy and imaging [13–16]. The purpose of loading anticancer drugs to the nanocarriers is to modulate the biodistribution profile of the drugs to the direction which is more favor for the cancer therapy with fewer side effects. Targeting functionalization of the nanocarrier's surface is one of the approaches to increase the accumulation of drug-loaded nanovectors to the targeted tissue area, as well as to possibly incorporate simultaneously imaging agents for cancer bioimaging. Both organic and inorganic nanomaterials have been investigated for cancer drug delivery [15]. Lipid-based nanosystems have produced the highest amount of cancer drug medicines in the market [13]. Liposomes have good biocompatibility, low immunogenicity, and biodegradability. The bilayer structure affords liposome to load both hydrophilic and hydrophobic drugs. Other amphiphilic nanoparticulate systems have also been investigated for cancer drug delivery, such as polymeric nanostructures (e.g., polymersomes, micelles, and dendrimers) [17, 18], and inorganic nanomaterials, including gold, single-/multi-wall carbon nanotubes, mesoporous silica, quantum dots, magnetic, and porous silicon (PSi) nanomaterials [19–23].

Among these nanosystems, PSi nanomaterials have presented attractive properties for anticancer drug delivery, such as good

biocompatibility, biodegradability, high drug loading, and turnable surface chemistry [20, 24–26]. PSi is made of crystalline elemental Si with nanosized pores structure. The surface of the crystalline silicon is highly reactive by hydrolysis and oxidation when exposing to the air [27]. After surface stabilization, the chemically active moieties, such as amine, carboxylic acid, and alkyne, can be introduced to the surface of PSi for further biofunctionalization [28–30]. Biofunctionalization of the nanovectors is a very interesting approach to enhance the nanovectors' interaction with the biological systems to profit the drug delivery, preventing unfavorable immune response, as well as to introduce imaging agents for diagnosis purpose [31–33].

Click chemistry was reported by Sharplees in 2001 as a simple method to couple organic molecules in high yields [34]. The features of click chemistry are the mild reaction conditions, high efficiency, and high specificity in the presence of a diverse range of functional groups [35]. The reactions are usually conducted at ambient conditions [36]. One of the most typical examples is the copper-catalyzed azide-alkyne cycloaddition (CuAAC) reaction. This CuAAC click reaction normally proceeds rapidly to completion and is highly selective due to the high thermodynamic driving force, which is usually greater than 20 kcal/mol [37]. Both reactive groups (azide and alkyne) are almost entirely inactive to other functional groups, such as amines, carboxylic acids, and hydroxyl, which widely exist in many bioactive molecules. The reaction avoids protection-deprotection steps and minimizes the side reactions. CuAAC is interesting for bioconjugation also due to the high reaction yield, the reaction selectivity/specificity, and the mild reaction conditions needed to preserve the bioactivity of biomolecules [38]. Strain-promoted azide-alkyne cycloaddition (SPAAC) click reaction, namely copper-free click reaction, becomes an alternative for the copper catalyzed click reaction [39, 40]. SPAAC avoids using the copper ion as a catalyst, which could induce cell and further in vivo biological toxicity. SPAAC has become an attractive tool for surface modification of biomaterials and coupling functional molecules to the nanovectors' surface for drug delivery and/or in vivo imaging applications [41, 42]. Bicyclononyne (BCN) and dibenzylcyclooctyne (DBCO) are two of the most commonly used moieties containing the strain-promoted cyclooctyne components [40]. The cyclooctane ring bent the triple bond into a geometry resembling the transition state of the cycloaddition reaction, and the electrophilic reaction with azide happens with low activation energy barrier [36]. Thus, the reaction can proceed at mild conditions.

This book chapter introduces the methods to conjugate peptides to PSi nanomaterials for peptide-mediated integrin-targeted anticancer drug delivery using SPAAC click chemistry. The protocols described herein include two methods to modify

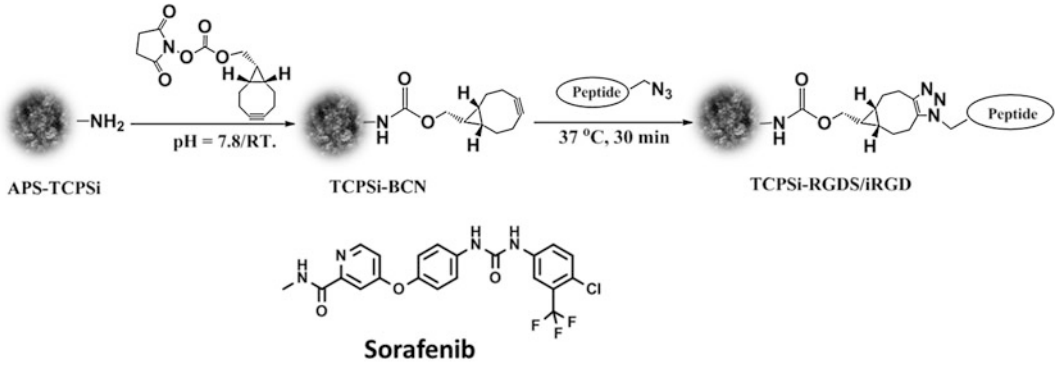

Scheme 1 The reaction routes of coupling SPAAC click moiety BCN to the amine-terminated PSi nanovector and further azide-functionalized RGDS and iRGD are conjugated to the surface of the nanovector via SPAAC. Reprinted with permission from Ref. [26]

both amine- and carboxylic acid-terminated PSi nanoparticles. In the first protocol, we describe the method to conjugate two RGD derivative peptides (one linear and one cyclized peptide sequence) to the amine-terminated PSi nanoparticles by two steps. In the first step, BCN is conjugated to the PSi through conventional amine-carboxylic acid reaction. In the second step, azide-terminated peptides are conjugated to BCN-decorated PSi nanoparticles by SPAAC click reaction (Scheme 1). In the second protocol, a multifunctional nanosystem is prepared based on the carboxylic acid-decorated PSi nanoparticles. To this system, simultaneously fluorescent labeling and radiolabeling for imaging, as well as iRGD modification for targeting, are incorporated to the surface of one single nanovector (Scheme 2).

2 Materials

All the commercially available solvents and reagents used in the protocols are used as received, without further purification or drying.

1. (1*R*,8*S*,9*s*)-bicyclo[6.1.0]non-4-yn-9-ylmethyl succinimidyl carbonate (BCN-NHS, Sigma-Aldrich, cat. no. 744867, stored at −20 °C; prepare a fresh solution before using).
2. Dibenzocyclooctyne-PEG4-amine (DBCO-PEG4-amine, Click Chemistry Tools, cat. no. A103P).
3. N-terminal azidoalanine-functionalized RGDS (RGDS-azide, GenicBio, custom order, stored at −20 °C as lyophilized powder; prepare a fresh solution before using).

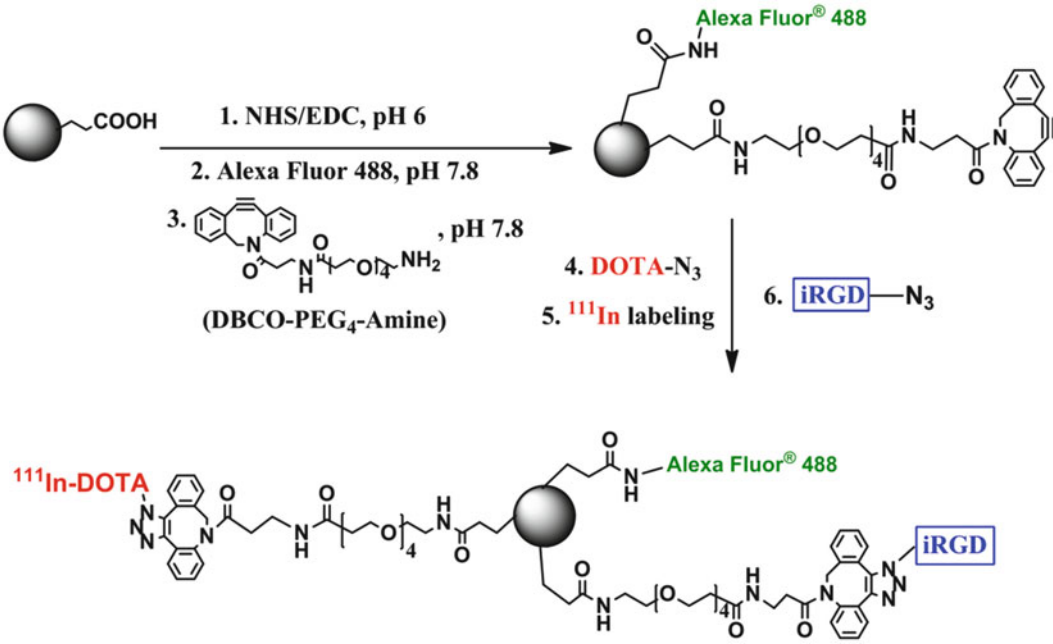

Scheme 2 Preparation of integrin-targeting peptide iRGD-modified multifunctional nanovectors for cancer theranostic. In reaction **step 1**, the carboxylic acid groups on the surface of PSi nanovectors are activated by EDC/NHS reaction. In reaction **step 2**, Alexa Fluor® 488 is conjugated to activate PSi nanovectors. In reaction **step 3**, SPAAC click moiety DBCO is linked to the surface of the PSi nanovectors (this step can be performed at the same time with reaction **step 2** as described in the protocol). In reaction **step 4**, the chelator DOTA is conjugated to the PSi nanovector via SPAAC click reaction. In reaction **step 5**, the radioactive tracer ^{111}In is incorporated to the PSi nanovectors (for more details of this step, please refer to Ref. [43]). In reaction **step 6**, the azide-functionalized peptide iRGD-azide is conjugated to the PSi nanovectors to form multifunctional nanovectors. Reprint with permission from Ref. [43]

4. N-terminal azidoalanine-functionalized iRGD (iRGD-azide, GenicBio, custom order, storage at −20 °C as lyophilized powder; prepare a fresh solution before using).
5. *N*,*N*-dimethylformamide (DMF, anhydrous, 99.8 %, Sigma-Aldrich, cat. no. 227056).
6. Amine-terminated PSi nanoparticles (customized prepared; Dr. Jarno Salonen, University of Turku).
7. Carboxylic acid-terminated PSi nanoparticles (customized prepared; Dr. Jarno Salonen, University of Turku).
8. 4-(2-hydroxyethyl)-1-piperazineethanesulfonic acid (HEPES, 99.5 %, titration, Sigma-Aldrich, cat. no. H3375).
9. Hydrogen chloride solution (1.0 M HCl, Sigma-Aldrich, cat. no. 318949).
10. Sodium hydroxide solution (5.0 M NaOH, Sigma-Aldrich, cat. no. S8263).

11. HEPES buffer (0.1 M, pH 7.8 or 5.5, prepared from HEPES powder; the pH is adjusted by 1.0 M HCl and 5.0 M NaOH).
12. *N*-(3-dimethylaminopropyl)-*N*′-ethylcarbodiimide hydrochloride (EDC, ≥98 %, Sigma-Aldrich, cat. no. 161462).
13. *N*-hydroxysuccinimide (NHS, 98 %, Sigma-Aldrich, cat. no. 130672).
14. Fluor Alexa® 488 hydrazide (Life Technologies, cat. no. A-10436).
15. 1,4,7,10-Tetraazacyclododecane-1,4,7-tris acetic acid-10-(azidopropyl-ethylacetamide) (Azido-mono-amide-DOTA, Macrocyclics Inc., cat. no. B-288).
16. Ethanol (EtOH, 99.5 %, Altia Corporation).
17. Milli-Q water.

3 Methods

3.1 RGD Derivative Peptides Conjugated to the Amine-Terminated PSi Nanovectors via SPAAC

In this section, the technique to modify the amine-terminated PSi nanovectors with integrin targeting peptides, RGDS and iRGD, is described [26]. This modification involves two steps of the PSi nanovector surface modification (Scheme 1). First, the SPAAC click moiety BCN is introduced to the amine-terminated PSi nanovector. Next, the azide-functionalized RGD derivative peptides, RGDS and iRGD, are linked to the nanovector by SPAAC click reaction.

3.1.1 Azide-Functionalized RGD Derivatives Preparation

The azide-functionalized RGDS and iRGD (RGDS-azide and iRGD-azide) are prepared by coupling an additional azidoalanine unit to the N-termini of the peptides RGDS and iRGD sequences. This synthesis is achieved through standard solid-support peptide synthesis (SSPS). The azidoalanine can tolerate the standard SSPS synthesis conditions and can be introduced to either the N- or C-terminal of the peptides. However, RGDS-azide and iRGD-azide can also be provided as custom serviced products by peptides synthesis suppliers, such as Sigma-Aldrich, GenicBio Ltd., United BioSystems Inc., and other commercial peptide suppliers. Our customized azide-functionalized peptides were obtained from GenicBio Ltd. Due to the possible instability of the peptides during the experimental procedure, it is recommended to store the peptides as lyophilized powder and prepare the peptide solutions freshly before every single use.

3.1.2 Cyclooctyne Functionalization of Amine-Terminated PSi Nanoparticles

1. Dissolve 3 mg of BCN-NHS in 400 μL anhydrous of DMF (**Note 1**).
2. Resuspend 2 mg of amine-terminated PSi nanoparticles in 400 μL of HEPES buffer (0.1 M, pH 7.8).

3. Add the dissolved BCN-NHS to PSi nanoparticles and keep the mixture under vigorous mixing at room temperature for 45 min.
4. Purify the BCN modified nanoparticles by transferring the reaction mixture to low-retention binding Eppendorf centrifuge tubes and concentrate the nanoparticles to pellet by centrifugation (Sorvall RC 5B plus, thermo Fisher Scientific, USA) at 10,000 × *g* for 3 min.
5. Discard the supernatant.
6. Wash the nanoparticles once with 1 mL of DMF/water (60/40 %, v/v), resuspend the pellet by tip sonication, centrifuge, and remove again the supernatant. Repeat the washing steps with Milli-Q water and ethanol.

The BCN-modified PSi nanoparticles can be resuspended in ethanol and stored at −20 °C and use during the following 1 week.

3.1.3 Peptide Conjugation to the Surface of PSi Nanoparticles via SPAAC Click Reaction

1. Weigh 0.5 mg of RGDS-azide or 1 mg iRGD-azide to the reaction glass vial (**Notes 2** and **3**).
2. Resuspend 1 mg of BCN-modified PSi nanoparticles in 500 µL of Milli-Q water and add to the vials containing the peptides. Protect the vials from light and place the vial in a shaker temperature controlled to 37 °C for 30 min.
3. Transfer the reaction mixture to low-retention binding Eppendorf centrifuge tubes and remove the reaction solution by centrifugation as described above.
4. Wash the reacted nanoparticles with 1 mL of ethanol/water (50/50 %, v/v), to remove the unreacted peptides.

The peptides modified nanovectors can be resuspended in ethanol and stored at −20 °C for further use (**Note 4**).

3.1.4 Characterization of the Surface Modification of the Nanoparticles

The chemical modification is followed step by step by Fourier transform infrared spectroscopy (FTIR) (Fig. 1). During the BCN modification and with both RGDS and iRGD conjugation, the amount of amide bond on the surface of the modified nanoparticles is significantly increased. Thus, the amide bonds (amide I at 1650 cm^{-1} and amide II at 1550 cm^{-1}) give specific signals in the FTIR spectrum, allowing to follow this reaction. The increase of signal intensity at the amide positions proves the successful conjugation onto the nanoparticle's surface at each step.

3.1.5 Enhanced Cellular Uptake

Benefiting from the specific affinity of RGD to the integrin receptors expressed by endothelial cells, our hypothesis is that RGD derivative peptides modification could enhance the cellular uptake of the PSi nanoparticles. The cellular uptake efficiency of the PSi nanoparticles before and after surface modification can be

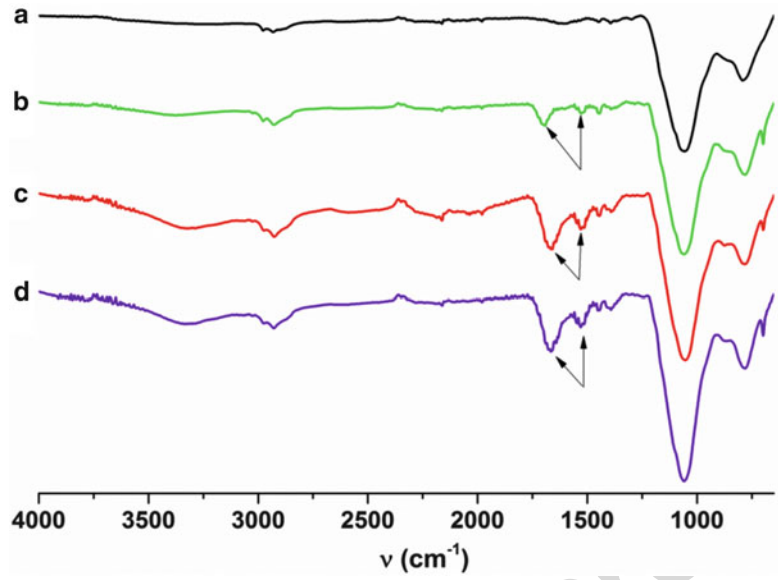

Fig. 1 FTIR spectra of amine-terminated PSi nanoparticles (*a*), and the BCN- (*b*), RGDS- (*c*), and iRGD- (*d*) conjugated PSi nanoparticles. *Arrows* indicate the amide positions (amide I at 1650 cm^{-1} and amide II at 1550 cm^{-1}). Adapted with permission from Ref. [26]

examined qualitatively by confocal fluorescent microscopy and quantitatively by flow cytometry analysis (Fig. 2). For this purpose, the PSi nanoparticles are fluorescent labeled, for example, by fluorescein isothiocyanate isomer I (FITC) prior to the peptides SPAAC click chemistry conjugation. The hybrid endothelial cell line EA.hy926 can be used for the cellular uptake studies. The results show that both RGDS and iRGD improves the cellular uptake of PSi nanoparticles. More specifically, the surface modification of the nanoparticles using RGDS enhances more efficiently the cellular uptake of the PSi nanoparticles than the iRGD modification. This might be due to the fact that there are more linear RGDS peptide units conjugated to the surface of PSi nanoparticles than for the cyclized iRGD peptides [26].

3.2 Peptide Conjugation to the Carboxylic Acid-Terminated PSi Nanovectors via SPAAC

In this section, carboxylic acid-terminated PSi nanoparticles are modified by SPAAC click conjugation (Scheme 2) with iRGD peptide [43]. Furthermore, by using this protocol both fluorescent labeling and radiolabeling are incorporated onto the surface of the same nanoparticle prior to the peptide attachment.

The azide-functionalized iRGD peptide is the same reagent as used in Section 3.1.

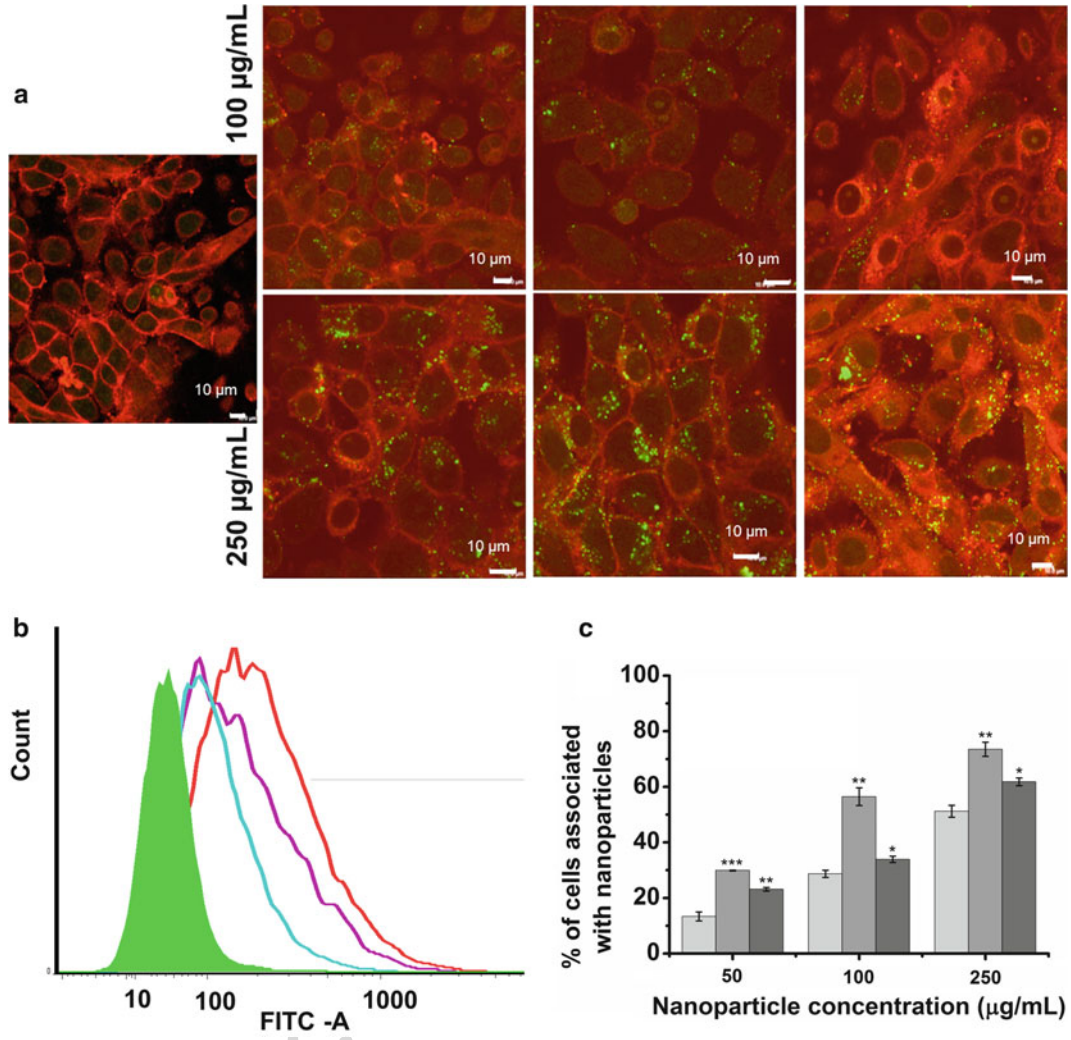

Fig. 2 Cellular uptake studies of RGD peptides modified amine-terminated PSi nanoparticles by confocal fluorescence microscopy and flow cytometry. (**a**) Confocal fluorescence microscopy images of endothelial cell EA.hy926 incubated with the RGD-modified PSi nanoparticles. The z-stack images represent the maximum intensity project of the PSi nanoparticles distribution in the cells. All three PSi nanoparticles were covalently labeled with FITC (*green color*) and the cell membrane was stained with CellMask™ (*orange color*). *First column* is the cell control. The *second*, *third*, and *forth columns* are the cells incubated with bare, RGDS- and iRGD-modified PSi nanoparticles, respectively. Scale bars are 10 µm. (**b**) Flow cytometry histograms of the cells incubated with the nanoparticles at the concentration of 250 µg/mL. *Solid green graphic*: cell control; the *blue graphic*: bare PSi nanoparticles; the *red graphic*: RGDS-modified PSi nanoparticles; and *purple graphic*: iRGD-modified PSi nanoparticles. (**c**) Cells that internalized nanoparticles determined by flow cytometry at three different concentrations. The *light grey*, *grey*, and *dark grey columns* represent bare, RGDS- and iRGD-modified PSi nanoparticles. The levels of the significant differences were set at probabilities of $*p < 0.05$ and $**p < 0.01$. Adapted with permission from Ref. [26]

3.2.1 Fluorescent Labeling and Dibenzylcyclooctyne Functionalization

Both fluorescent dye Alexa Fluor® 488 and DBCO are covalently linked to the PSi nanoparticles using an EDC/NHS reaction.

1. Dissolve 3 mg of NHS and 2 μL of EDC in 2 mL of HEPES buffer (0.1 M, pH 5.5).
2. Add 1 mg of carboxylic acid-terminated PSi nanoparticles in 1 mL ethanol to the solution and keep stirring for 30 min at room temperature.
3. Conjugate the Alexa Fluor® 488 and the DBCO moiety to the surface of PSi nanoparticles. For this, dissolve 1 mg of DBCO-PEG4-amine in 200 μL of DMF and the Alexa Fluor® 488 in Milli-Q water with a concentration of 0.5 mg/mL (**Note 5**).
4. Add 1 mg of DBCO-PEG4-amine and 10 μg of Alexa Fluor® 488 to the activated PSi nanoparticle solution.
5. Adjust the pH of the reaction mixture to 7.8 with 1 M NaOH. Protect the reaction vial from the light.
6. After 1-h reaction, harvest the nanoparticles by centrifugation at 10,000 × *g* for 3 min, and wash the nanoparticles three times with 1 mL of DMF, water, and ethanol in the same way as described in Section 3.1.4.

The Alexa Fluor® 488-labeled DBCO modified PSi nanoparticles can be stored in ethanol at −20 °C for further use.

3.2.2 DOTA Conjugation to the Surface of the PSi Nanoparticles via SPAAC

DOTA can be used for radiolabeling by chelating the radioactive ion ^{111}Indium (^{111}In) or as contrast regents by complexing with gadolinium (Gd^{3+}) [44].

1. Dissolve 1 mg of azide-functionalized DOTA in 1 mL of DMF (**Note 6**). Control the amount of DOTA that can be conjugated to the surface of the PSi nanoparticles.
2. Add 10 μg of DOTA solution to the vial containing 1 mg of the DBCO functionalized PSi nanoparticles in 1 mL of Milli-Q water. Protect the vial from light by covering the glass vial with foil paper.
3. Keep the reaction mixture on a shaker at 37 °C for 30 min.
4. After reaction, collect the nanoparticles by centrifugation (the same procedure as described in Section 3.1.4) and discard the supernatant.
5. Remove the unreacted DOTA by washing once with DMF and twice with ethanol to obtain DOTA decorated PSi nanoparticles.

The modified nanoparticles can be stored in ethanol at −20 °C for further use.

The nanovector can be radiolabeled through DOTA moiety chelating radioactive ion ^{111}In [43]. By controlling the reaction

ratio of DOTA to the DBCO-modified PSi nanovector, there are free DBCO groups on the surface of the PSi nanovector which can be further used for peptide conjugation via SPAAC click chemistry.

3.2.3 iRGD Conjugation to Fluorescent-Labeled and DOTA-Decorated PSi Nanoparticles via SPAAC

1. Weigh 1 mg of azidoalanine-iRGD (iRGD-azide) in a glass vial.
2. Add 1 mg of DOTA decorated PSi nanoparticles (product from **step 3** in Section 3.2.2) suspended in Milli-Q water to the glass vial containing iRGD-azide. Protect the reaction from light by covering the glass vial with foil paper.
3. Place the reaction mixture at 37 °C for 1 h with shaking.
4. After reaction, harvest the nanoparticles by centrifugation as described in Section 3.1.4, and wash the nanoparticles with 1 mL ethanol/water (50/50 %, v/v), to remove the unreacted peptides.

The peptide-conjugated nanovectors can be stored in ethanol at −20 °C for further use (**Note 4**).

3.2.4 Characterization of the Modified PSi Nanovectors

In this protocol, all the modification steps are monitored by FTIR (Fig. 3). The increase signal intensity of amide I (1650 cm^{-1}) and amide II (1550 cm^{-1}) in the FTIR spectra shows that Alexa Fluor®

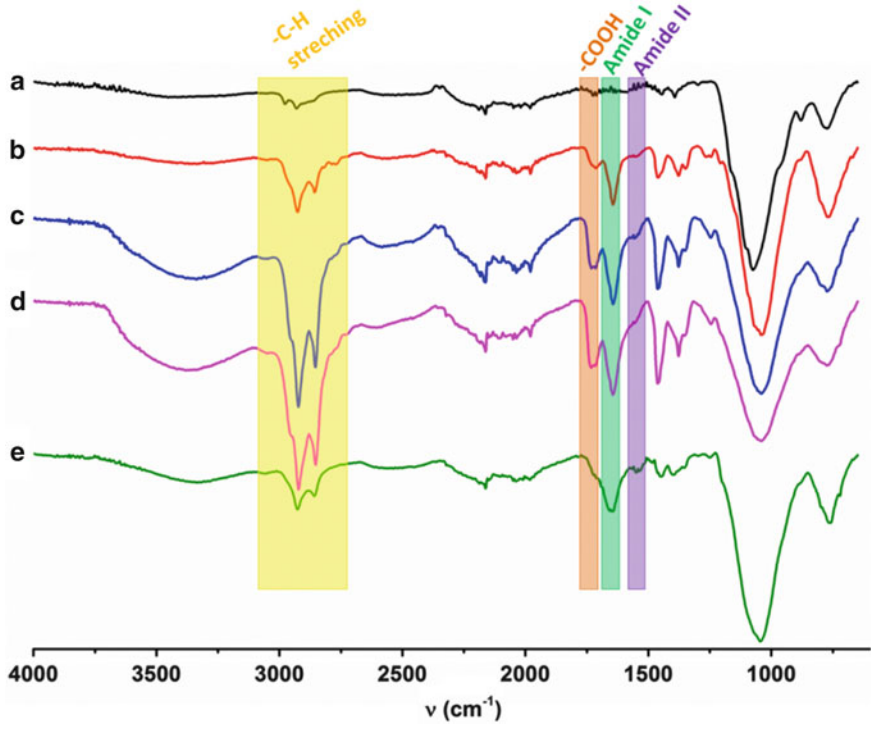

Fig. 3 FTIR spectra of carboxylic acid-terminated PSi nanoparticles (*a*) and the nanoparticles with each step modification: Alexa Fluor® 488 (*b*); Alexa Fluor® 488 and DBCO (*c*); Alexa Fluor® 488, DBCO, and DOTA (*d*): and Alexa Fluor® 488, DBCO, DOTA, and iRGD (*e*). Adapted with permission from Ref. [43]

488 and DBCO are conjugated to the carboxylic acid-terminated PSi nanoparticles via an amide linkage (Fig. 3b, c). The bands observed in the region of 2800–2960 cm^{-1} correspond to the C–H stretching, confirming the conjugation of the DBCO moiety containing four ethylene glycol units. After DOTA conjugation, the carboxylic acid peak at 1720 cm^{-1} is increased. By the iRGD conjugation onto the PSi nanoparticle's surface, the amide peaks are strengthened. On the other hand, the carboxylic acid and C–H stretching are decreased, which is properly due to the presence of the peptide iRGD, seen as increased signal intensity in the amide bands. This indicates the successful conjugation of Alexa Fluor® 488, DOTA, and iRGD to the surface of PSi nanoparticles.

3.2.5 *In Vivo Tumor Targeting Efficiency of iRGD-Modified Nanoparticles*

The integrin biomarkers are actively expressed during tumor neovascularization [3]. The iRGD peptide has been successfully used to enhance the delivery efficiency of nanovectors to the tumor site [9, 10, 45]. The in vivo tumor targeting efficiency of the PSi nanoparticles after the conjugation of iRGD to the surface of the nanovector via SPAAC can also be evaluated as shown in Fig. 4 [43]. The bare and iRGD-modified PSi nanoparticles were labeled by a radioactive agent ^{111}In in order to allow the quantification of the tumor accumulation of the nanoparticles. The nanoparticles were then intravenously administered into a xenograft mice model. The results showed that compared to the PSi nanoparticles without iRGD conjugation, iRGD-modified PSi nanoparticles induced higher tumor-specific accumulation.

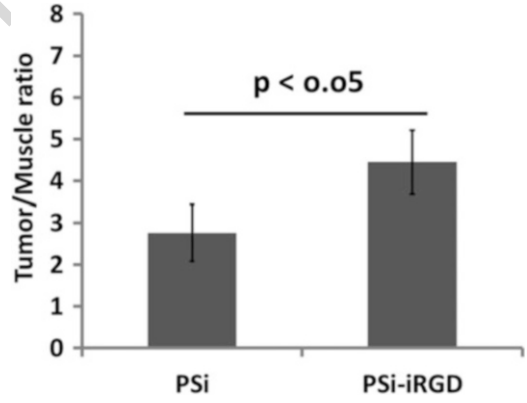

Fig. 4 Tumor accumulation of the PSi nanoparticles without iRGD conjugation (designated as PSi in the figure) and with iRGD surface modification (designated as PSi-iRGD in the figure). The nanoparticles were administered intravenously and the organs were harvest 27 h post-injection. The radioactivity of each organ was determined by gamma-counting analysis. Adapted with permission from Ref. [43]

4 Notes

1. Depending on the scale of the reaction, the amount of BCN-NHS and DMF can be changed, but it is important to keep this ratio as well as the ratio of DMF to the amount of aqueous buffer used during the step of addition of the PSi nanoparticles. This is due to the solubility limitation of BCN-NHS in DMF/water solution.
2. Lyophilized powder of the peptides can be stored at −20 °C. Open the vials when the temperature of the peptide vials equals to room temperature and weigh the amount of peptides powder needed every time before using them.
3. In this reaction, the amount of peptides used is in excess compared to the available group of BCN on the surface of the PSi nanoparticles.
4. The degradation of the peptides depends on the sequence and the solutions used. There is no evidence that the RGD peptides used in these protocols will be degraded very fast in ethanol at −20 °C, but for quality control purpose, it is recommended to use the peptide-modified nanovectors as freshly as possible. This is also one of the reasons the SPAAC click reaction method is chosen in order to get the surface of the nanoparticles modified with the peptides in a fast process with a high yield.
5. Alexa Fluor® 488 hydrazine can be dissolved in Milli-Q water and stored as aliquots at −20 °C up to several months.
6. DOTA-azide can be dissolved in DMF and stored as aliquots at −20 °C up to several months.

Acknowledgements

Financial support from Academy of Finland (decision nos. 252215 and 281300), University of Helsinki Research Funds, Biocentrum Helsinki, and European Research Council (grant no. 310892).

References

1. Hanahan D, Weinberg RA (2011) Hallmarks of cancer: the next generation. Cell 144 (5):646–674
2. Hanahan D, Folkman J (1996) Patterns and emerging mechanisms of the angiogenic switch during tumorigenesis. Cell 86(3):353–364
3. Ruoslahti E, Bhatia SN, Sailor MJ (2010) Targeting of drugs and nanoparticles to tumors. J Cell Biol 188(6):759–768
4. Ruoslahti E (2002) Specialization of tumour vasculature. Nat Rev Cancer 2(2):83–90
5. Brooks PC, Clark RA, Cheresh DA (1994) Requirement of vascular integrin alpha v beta 3 for angiogenesis. Science 264 (5158):569–571
6. Weis SM, Cheresh DA (2011) alphaV integrins in angiogenesis and cancer. Cold Spring Harb Perspect Med (1):a006478

7. Pierschbacher MD, Ruoslahti E (1984) Cell attachment activity of fibronectin can be duplicated by small synthetic fragments of the molecule. Nature 309(5963):30–33
8. Pierschbacher MD, Ruoslahti E (1984) Variants of the cell recognition site of fibronectin that retain attachment-promoting activity. Proc Natl Acad Sci U S A 81(19):5985–5988
9. Shen J, Meng Q, Sui H, Yin Q, Zhang Z, Yu H, Li Y (2014) iRGD conjugated TPGS mediates codelivery of paclitaxel and survivin shRNA for the reversal of lung cancer resistance. Mol Pharm 11(8):2579–2591
10. Sugahara KN, Teesalu T, Karmali PP, Kotamraju VR, Agemy L, Greenwald DR, Ruoslahti E (2010) Coadministration of a tumor-penetrating peptide enhances the efficacy of cancer drugs. Science 328(5981):1031–1035
11. Chen CW, Lu DW, Yeh MK, Shiau CY, Chiang CH (2011) Novel RGD-lipid conjugate-modified liposomes for enhancing siRNA delivery in human retinal pigment epithelial cells. Int J Nanomedicine 6:2567–2580
12. Sugahara KN, Teesalu T, Karmali PP, Kotamraju VR, Agemy L, Girard OM, Hanahan D, Mattrey RF, Ruoslahti E (2009) Tissue-penetrating delivery of compounds and nanoparticles into tumors. Cancer Cell 16 (6):510–520
13. Allen TM, Cullis PR (2013) Liposomal drug delivery systems: from concept to clinical applications. Adv Drug Deliv Rev 65(1):36–48
14. Couvreur P (2013) Nanoparticles in drug delivery: past, present and future. Adv Drug Deliv Rev 65(1):21–23
15. Gao Y, Xie J, Chen H, Gu S, Zhao R, Shao J, Jia L (2014) Nanotechnology-based intelligent drug design for cancer metastasis treatment. Biotechnol Adv 32(4):761–777
16. Luk BT, Zhang L (2014) Current advances in polymer-based nanotheranostics for cancer treatment and diagnosis. ACS Appl Mater Interfaces 6(24):21859–21873
17. Bai F, Wang C, Lu Q, Zhao M, Ban FQ, Yu DH, Guan YY, Luan X, Liu YR, Chen HZ, Fang C (2013) Nanoparticle-mediated drug delivery to tumor neovasculature to combat P-gp expressing multidrug resistant cancer. Biomaterials 34(26):6163–6174
18. Bigini P, Previdi S, Casarin E, Silvestri D, Violatto MB, Facchin S, Sitia L, Rosato A, Zuccolotto G, Realdon N, Fiordaliso F, Salmona M, Morpurgo M (2014) In vivo fate of avidin-nucleic acid nanoassemblies as multifunctional diagnostic tools. ACS Nano 8(1):175–187
19. Prasad P, Gordijo CR, Abbasi AZ, Maeda A, Ip A, Rauth AM, DaCosta RS, Wu XY (2014) Multifunctional albumin-MnO(2) nanoparticles modulate solid tumor microenvironment by attenuating hypoxia, acidosis, vascular endothelial growth factor and enhance radiation response. ACS Nano 8(4):3202–3212
20. Bimbo LM, Sarparanta M, Santos HA, Airaksinen AJ, Mäkilä E, Laaksonen T, Peltonen L, Lehto VP, Hirvonen J, Salonen J (2010) Biocompatibility of thermally hydrocarbonized porous silicon nanoparticles and their biodistribution in rats. ACS Nano 4 (6):3023–3032
21. Lee SM, Kim HJ, Kim SY, Kwon MK, Kim S, Cho A, Yun M, Shin JS, Yoo KH (2014) Drug-loaded gold plasmonic nanoparticles for treatment of multidrug resistance in cancer. Biomaterials 35(7):2272–2282
22. Al-Jamal KT, Nunes A, Methven L, Ali-Boucetta H, Li S, Toma FM, Herrero MA, Al-Jamal WT, ten Eikelder HM, Foster J, Mather S, Prato M, Bianco A, Kostarelos K (2012) Degree of chemical functionalization of carbon nanotubes determines tissue distribution and excretion profile. Angew Chem Int Ed Engl 51(26):6389–6393
23. Li C, Yang D, Ma P, Chen Y, Wu Y, Hou Z, Dai Y, Zhao J, Sui C, Lin J (2013) Multifunctional upconversion mesoporous silica nanostructures for dual modal imaging and in vivo drug delivery. Small 9(24):4150–4159
24. Salonen J, Laitinen L, Kaukonen AM, Tuura J, Bjorkqvist M, Heikkilä T, Vaha-Heikkilä K, Hirvonen J, Lehto VP (2005) Mesoporous silicon microparticles for oral drug delivery: loading and release of five model drugs. J Control Release 108(2–3):362–374
25. Santos HA, Bimbo LM, Lehto VP, Airaksinen AJ, Salonen J, Hirvonen J (2011) Multifunctional porous silicon for therapeutic drug delivery and imaging. Curr Drug Discov Technol 8 (3):228–249
26. Wang CF, Mäkilä EM, Kaasalainen MH, Liu D, Sarparanta MP, Airaksinen AJ, Salonen JJ, Hirvonen JT, Santos HA (2014) Copper-free azide-alkyne cycloaddition of targeting peptides to porous silicon nanoparticles for intracellular drug uptake. Biomaterials 35 (4):1257–1266
27. Canham LT, Saunders SJ, Heeley PB, Keir AM, Cox TI (1994) Rapid chemography of porous silicon undergoing hydrolysis. Adv Mater 6 (11):865–868
28. Mäkilä E, Bimbo LM, Kaasalainen M, Herranz B, Airaksinen AJ, Heinonen M, Kukk E, Hirvonen J, Santos HA, Salonen J (2012) Amine modification of thermally carbonized porous silicon with silane coupling chemistry. Langmuir 28(39):14045–14054

29. Kovalainen M, Mönkäre J, Kaasalainen M, Riikonen J, Lehto VP, Salonen J, Herzig KH, Järvinen K (2013) Development of porous silicon nanocarriers for parenteral peptide delivery. Mol Pharm 10(1):353–359
30. Wang CF, Mäkilä EM, Bonduelle C, Rytkönen J, Raula J, Almeida S, Närvänen A, Salonen JJ, Lecommandoux S, Hirvonen JT, Santos HA (2015) Functionalization of alkyne-terminated thermally hydrocarbonized porous silicon nanoparticles with targeting peptides and antifouling polymers: effect on the human plasma protein adsorption. ACS Appl Mater Interfaces 7(3):2006–2015
31. Egli S, Nussbaumer MG, Balasubramanian V, Chami M, Bruns N, Palivan C, Meier W (2011) Biocompatible functionalization of polymersome surfaces: a new approach to surface immobilization and cell targeting using polymersomes. J Am Chem Soc 133(12):4476–4483
32. Krasnici S, Werner A, Eichhorn ME, Schmitt-Sody M, Pahernik SA, Sauer B, Schulze B, Teifel M, Michaelis U, Naujoks K, Dellian M (2003) Effect of the surface charge of liposomes on their uptake by angiogenic tumor vessels. Int J Cancer 105(4):561–567
33. Sapsford KE, Algar WR, Berti L, Gemmill KB, Casey BJ, Oh E, Stewart MH, Medintz IL (2013) Functionalizing nanoparticles with biological molecules: developing chemistries that facilitate nanotechnology. Chem Rev 113 (3):1904–2074
34. Kolb HC, Finn MG, Sharpless KB (2001) Click chemistry: diverse chemical function from a few good reactions. Angew Chem Int Ed Engl 40(11):2004–2021
35. Xi W, Scott TF, Kloxin CJ, Bowman CN (2014) Click chemistry in materials science. Adv Funct Mater 24(18):2572–2590
36. Ess DH, Jones GO, Houk KN (2008) Transition states of strain-promoted metal-free click chemistry: 1,3-dipolar cycloadditions of phenyl azide and cyclooctynes. Org Lett 10 (8):1633–1636
37. Lallana E, Sousa-Herves A, Fernandez-Trillo F, Riguera R, Fernandez-Megia E (2012) Click chemistry for drug delivery nanosystems. Pharm Res 29(1):1–34
38. Sawoo S, Dutta P, Chakraborty A, Mukhopadhyay R, Bouloussa O, Sarkar A (2008) A new bio-active surface for protein immobilisation via copper-free 'click' between azido SAM and alkynyl Fischer carbene complex. Chem Commun 7(45):5957–5959
39. Sletten EM, Bertozzi CR (2011) From mechanism to mouse: a tale of two bioorthogonal reactions. Acc Chem Res 44(9):666–676
40. Debets MF, van Berkel SS, Dommerholt J, Dirks AT, Rutjes FP, van Delft FL (2011) Bioconjugation with strained alkenes and alkynes. Acc Chem Res 44(9):805–815
41. Chen K, Wang X, Lin WY, Shen CK, Yap LP, Hughes LD, Conti PS (2012) Strain-promoted catalyst-free click chemistry for rapid construction of ^{64}Cu-labeled PET imaging probes. ACS Med Chem Lett 3(12):1019–1023
42. Lee DE, Na JH, Lee S, Kang CM, Kim HN, Han SJ, Kim H, Choe YS, Jung KH, Lee KC, Choi K, Kwon IC, Jeong SY, Lee KH, Kim K (2013) Facile method to radiolabel glycol chitosan nanoparticles with ^{64}Cu via copper-free click chemistry for microPET Imaging. Mol Pharm 10(6):2190–2198
43. Wang CF, Sarparanta MP, Mäkilä EM, Hyvonen ML, Laakkonen PM, Salonen JJ, Hirvonen JT, Airaksinen AJ, Santos HA (2015) Multifunctional porous silicon nanoparticles for cancer theranostics. Biomaterials 48:108–118
44. Li S, Goins B, Zhang L, Bao A (2012) Novel multifunctional theranostic liposome drug delivery system: construction, characterization, and multimodality MR, near-infrared fluorescent, and nuclear imaging. Bioconjug Chem 23 (6):1322–1332
45. Su S, Wang H, Liu X, Wu Y, Nie G (2013) iRGD-coupled responsive fluorescent nanogel for targeted drug delivery. Biomaterials 34 (13):3523–3533